MASTER'S THESIS 2024

# Flanking sound transmission over CLT-joints

Eric Andersson

Department of Civil and Environmental Engineering
*Division of Applied Acoustics*
*Roomacoustics Group or Vibroacoustics Group*
CHALMERS UNIVERSITY OF TECHNOLOGY
Göteborg, Sweden 2024

Flanking sound transmission over CLT-joints



Master's Thesis 2024

Department of Civil and Environmental Engineering
Division of Applied Acoustics
Roomacoustics Group or Vibroacoustics Group
Chalmers University of Technology
SE-41296 Göteborg
Sweden

Tel. +46-(0)31 772 1000

Reproservice / Department of Civil and Environmental Engineering
Göteborg, Sweden 2024

Flanking sound transmission over CLT-joints
Master's Thesis in the Master's programme in Sound and Vibration
Eric Andersson
Department of Civil and Environmental Engineering
Division of Applied Acoustics
Roomacoustics Group or Vibroacoustics Group
Chalmers University of Technology

## Abstract

Cross-laminated timber (CLT) is a sustainable and efficient building material that has gained popularity due to its high stiffness, low density, and reduced environmental impact. However, predicting low-frequency sound and vibration transmission across CLT joints remains a significant challenge. This thesis focuses on improving the modeling of flanking sound transmission over different CLT joint configurations, using finite element modeling (FEM) validated through experimental measurements. The study involves measurements of vibration reduction index ($K_{ij}$) for undamped and isolated joint setups. The FEM simulations closely matched experimental trends for non isolated setups, though some discrepancies arose due to possible differences in coupling conditions and measurement resolution. In isolated setups, FEM predictions highlighted limitations in accurately simulating the effect of vibration-isolation brackets, particularly in representing their behavior when fastened to the CLT panels.
The results emphasize the need for refined FEM approaches to better model the dynamic behavior of joints and connections in CLT structures. Future work should focus on enhancing joint coupling simulations, modeling of vibration-isolation brackets and optimizing experimental setups to achieve free boundary conditions. Thereby advancing the acoustic performance prediction for CLT constructions.

# Contents

# Acknowledgements

I would like to express my heartfelt gratitude to everyone who contributed to the successful completion of this work.
First and foremost, I am deeply grateful to my supervisors, Krister Larsson and Andreas Colebring, for their invaluable guidance, encouragement, and support throughout the project. Their expertise and constructive feedback were instrumental in shaping this thesis.
I extend my sincere thanks to Afry (Efterklang) and Chalmers for providing the resources and facilities necessary to carry out this work. I am also thankful to my colleagues and peers for their insightful discussions and unwavering support.
I would like to specially thank Sebastian Almfeldt and Nicklas Vallström for their assistance in the structures lab, which was essential for the experimental aspects of this project.
I would also like to express my gratitude to my examiner, Jens Forssén, for their valuable time, thorough review, and constructive feedback, which greatly improved the quality of this thesis.
A special thanks goes to my family and friends for their endless encouragement and patience throughout this journey. Their belief in me has been a constant source of strength.
Finally, I wish to acknowledge Christian Berner, Vibratec, and Rothoblaas for their generous contributions, which were vital in making this project possible.

# Chapter 1

# Introduction

## 1.1 Background

Cross laminated timber (CLT) has gained popularity in the building industry due to its unique combination of high stiffness and low density. The material offers good seismic resistance, facilitates easy construction of various building elements, and has a lower environmental impact compared to concrete. However, a challenge arises in accurately predicting how low-frequency noise and vibrations, especially within joints, affect CLT panels. Existing practices involve using elastic layers in joints, often unnecessarily, as these practices are designed for concrete rather than wood-based CLT panels.
This study aims to develop a more precise model for predicting transmission across joints in CLT panels, with the goal of reducing the reliance on elastic materials in joints. This not only cuts costs but also minimizes material waste, a crucial consideration as CLT panels become more popular in construction, aligning with growing environmental concerns. Utilizing fewer materials further supports eco-friendly practices by reducing overall production needs.(3)

## 1.2 Cross laminated timber

CLT panels are constructed by gluing wooden planks together and layering these slabs, typically five to seven layers deep, with the grain direction alternating between each layer. These panels range in thickness from 80 mm to 300 mm, with widths between 1.2 m and 3 m, and lengths up to 16 m.

Due to their significantly lower weight compared to concrete, CLT panels are easier to handle, allowing for pre-fabrication and efficient transportation to construction sites. The reduced weight also eliminates the need for reinforced foundations to the same extent required for materials like concrete.
CLT panels are inherently orthotropic, with material properties varying depending on the direction. This differs from isotropic materials with consistent properties throughout. The orthotropic nature of CLT panels is influenced by the number of layers of wooden slabs used in their construction.
While CLT panels possess high strength relative to their weight, they do face challenges in low-frequency insulation. Acoustically, they may not handle low-frequency noise as effectively.(3)

## 1.3 Aim

The aim of this thesis is to develop a FEM model that is better at predicting low frequency flanking transmissions over cross laminated timber (CLT) joints than the existing tools, which will help to determine if damping materials such as sylomers are needed for the joints or not. The joints that are to be studied are T-joints and X-joints.

## 1.4 Method

Due to the nature of flanking transmission being a quite complicated issue where several factors needs to be considered numerical calculations will not be reliable enough due to simplifications. Instead Finite Element Modelling (FEM) will be used which is a deterministic approach. FEM is the best simulation method in this case as it focuses on the low frequency range where FEM is more reliable.
The flanking sound transmission will then be measured on CLT panels for different joint setups, such as L-joints T-joints and X-joints. The measurements will then be compared to the FEM results to validate the simulation.

# Chapter 2

# Theory

## 2.1 Waves in solids

Waves in solids are very different from waves in fluids, due to the shear stresses and shear deformations that occur. Because of this other wave types are seen besides longitudinal waves. In an infinite structure, two different types of waves can propagate simultaneously, longitudinal waves and ideal transversal or shear waves. For transversal and shear waves the particles move in the direction of the wave propagation. From the elastic equations it is possible to show that the wave motion in solids can be seen as a combination of the waves mentioned before. (2) (4)

### 2.1.1 Longitudinal waves

In reality, longitudinal waves do not truly exist because they require infinite structures, which do not occur in practical scenarios. Instead in an actual structure a longitudinal wave will cause a lateral displacement on the surface. This type of wave is called a quasi-longitudinal wave. The wave speed of such a wave propagating in one direction can be calculated as:

$$c_L = \sqrt{\frac{E'}{\rho}} \tag{2.1}$$

where $E'$ is the Young's modulus in pascals $\rho$ is the material density in $kg/m^3$. When the wave is propagating through a plate it occurs in two directions $x$ and $y$. This relationship of the strains caused in the material can then be described as following: (2) (4)

$$|\epsilon_x| = v|\epsilon_y| \tag{2.2}$$

where $v$ is Poisson's ratio. $E'$ can then be written as:

$$E' = \frac{E}{1 - v^2} \tag{2.3}$$

The speed for a longitudinal wave can then be expressed as:

$$c_{L(x,y)} = \sqrt{\frac{E}{\rho(1 - v^2)}} \tag{2.4}$$

### 2.1.2 Shear waves

In a pure shear wave, also known as a transverse wave there is only shear deformations and no change in volume. The particles movements are in the normal direction of the wave propagation. To calculate the shear wave speed the shear modulus first needs to be calculated which can be done using: (2) (4)

$$G = \frac{E}{2(1 + v)} \tag{2.5}$$

and then to calculate the speed ($c_S$):

$$c_S = \sqrt{\frac{G}{\rho}} \tag{2.6}$$

Then with equations 2.4, 2.5 and 2.6 the equation for a plate becomes:

$$\frac{c_S}{c_L} = \sqrt{\frac{1 - v}{2}} \tag{2.7}$$

### 2.1.3 Bending waves

Bending waves (flexural waves) will likely appear in structures where the dimensions are becoming small in comparison to the wave length.
Because these waves are easily excited and are dominant in common construction elements such as plates they are very important in building acoustics.
Just like the shear waves the particle velocity will be normal to the direction of propagation, which means that that it will be normal to the surface of the element. This in turn will cause the element to have a strong coupling to the surrounding air this means that the element could be an efficient sound source.

To calculate bending waves simplifications are usually applied. According to the Euler Bernoulli theory the bending angle can be calculated using: (2) (4)

$$\beta = \frac{\partial \eta}{\partial x} \tag{2.8}$$

where $\eta$ is the displacement in the normal direction and $x$ is the position on the x-axle. The bending moment can then be described as:

$$M = -B\frac{\partial \beta}{\partial x} = -B\frac{\partial^2 \eta}{\partial x^2} \tag{2.9}$$

where $B$ is bending stiffness. If 2 different moments were to be applied to the ends the difference in moment will lead to a net force which can be calculated as following:

$$F = -\frac{\partial M}{\partial x} = \frac{\partial}{\partial x} B\frac{\partial^2 \eta}{\partial x^2} \tag{2.10}$$

The force also changes along the length of the beam ($x$). A particle will accelerate due to the net force being applied to it, therefor newtons law will lead to:

$$-\frac{\partial F}{\partial x} = m\frac{\partial^2 \eta}{\partial x^2} \tag{2.11}$$

where ($m$) is the mass per unit length $(\rho S)$. The wave equation can be acquired by combining equation 2.10 and 2.11:

$$\frac{\partial^2}{\partial x^2}\left(B(x)\frac{\partial^2 \eta}{\partial x^2}\right) + m\frac{\partial^2 \eta}{\partial t^2} \tag{2.12}$$

Assuming constant bending stiffness equation 2.12 can be simplified to:

$$B\frac{\partial^4 \eta}{\partial x^4} + m\frac{\partial^2 \eta}{\partial t^2} = 0 \tag{2.13}$$

The solution then needs to be written in wave form $\eta(x,t) = \eta_A e^{-jkx} e^{jwt}$ the equation above can be written as:

$$(Bk^4 - \omega^2 m)\eta_A = 0 \tag{2.14}$$

equation 2.14 can then be simplified as:

$$k^4 = \frac{\omega^2 m}{B} \tag{2.15}$$

where $k$ is the wave number of the bending waves.

With equation 2.15 and the equation for the speed of sound we can express the wave speed for a bending wave as:

$$c_B = \sqrt[4]{\frac{B}{m}\omega^2} \tag{2.16}$$

where $m$ can be calculated as:

$$m = \rho h \tag{2.17}$$

The bending stiffness ($B$) can be expressed with the following equation:

$$B = \frac{Eh^3}{[12(1-\nu^2)]} \tag{2.18}$$

where $h$ is the thickness of the plate.(5)

## 2.2 Modal analysis

Each structural configuration exhibits unique responses, dictated by its shape and the constraints imposed by boundary conditions. Specific frequencies induce more pronounced reactions within the structure, attributable to its inherent natural frequencies, which define characteristic modes of motion. Analyzing these individual modes facilitates a deeper understanding of structural behavior. (4)

#### Isotropic plates

The eigenfrequencies of an isotropic simply supported plate can be calculated by first visualizing the plate as two beams, one along the x-axis and another along the y-axis. The wave number for a beam can be described as:

$$k_B^2 = \left(\frac{p\pi}{L_x}\right)^2 \tag{2.19}$$

Where $L_x$ is the length of the beam in meters and $p$ is a positive integer. The wave number for modes in thin plates can then be described as (4):

$$k_B^2 = \left(\frac{p\pi}{L_x}\right)^2 + \left(\frac{q\pi}{L_y}\right)^2 \tag{2.20}$$

Where $p$ and $q$ are the mode numbers. By then combining the above equation with 2.15 the eigenfrequencies can be calculated using the following equation (4):

$$f_{pq} = \frac{\pi}{2}\sqrt{\frac{B}{m}}\left[\left(\frac{p}{L_x}\right)^2 + \left(\frac{q}{L_y}\right)^2\right] \tag{2.21}$$

**Orthotropic plates**

Cross laminated timber is in reality an anisotropic material. This means that the material properties change depending on the direction of the material, this is because of the grain direction in the wood that the CLT panels are made out of. An orthotropic material is closer to an anisotropic material than the isotropic material, orthotropic materials has different material parameters such as Young's modulus Poisson's ratio and shear modulus in the x-, y- and z-directions. Because of this the bending stiffness for orthotropic materials differ from each other depending on the direction. The bending stiffness can be calculated using the following equations: (11)

$$B_x = \frac{E_x h^3}{12(1 - v_x v_y)} \tag{2.22}$$

$$B_y = \frac{E_y h^3}{12(1 - v_x v_y)} \tag{2.23}$$

The eigenfrequencies can then be calculated using:

$$f_{pq} = \frac{\pi}{2\sqrt{m}} \left[ \sqrt{B_x} \left( \frac{p}{L_x} \right)^2 + \sqrt{B_y} \left( \frac{q}{L_y} \right)^2 \right] \tag{2.24}$$

## 2.3 Flanking transmission

Flanking transmission refers to the transfer of sound or vibration between spaces through indirect paths, rather than directly through the separating element. To be able to analyse the vibration transmission the transmission coefficient can be calculated using the following equation:

$$\tau_{ij} = \frac{W_{ij}}{W_{inc,i}} \tag{2.25}$$

Where $W_{ij}$ is the power transmitted across the junction (the point of contact between two elements) and $W_{inc,i}$ is the incident power. The transmission loss can then be converted to a decibel scale using:

$$Tl = 10log(\frac{1}{\tau_{ij}}) \tag{2.26}$$

The wave method assumes a specific angle, $\theta$ for incidence. This means the transmission coefficient $\tau_{ij}$, depends on the angle. However, when vibrations are scattered (above the first eigenfrequency), all angles of

incidence are equally likely. So to estimate the average transmission coefficient across angles we can use the normal transmission coefficient. Also, when transmission occurs across a joint it follows Snell's law which relates the angle of incidence to the angle of transmission. (4)

$$k_i sin(\theta_i) = k_j sin(\theta_j) \tag{2.27}$$

where $\theta_i$ is the angle of incidence and $\theta_j$ is the angle of transmission.

## 2.4 Vibration reduction index

CLT, categorized as a form of solid wood product, is classified as a Type A element according to ISO 10848-1 standards. The primary parameter utilized for assessing vibration transmission across CLT joints is the vibration reduction index $(K_{ij})$. This index, as outlined in ISO 12354-1, serves as a consistent measure to evaluate the transmission of vibrational power between structural components at junctions. $K_{ij}$ is determined through structural-borne excitation and involves normalizing the direction-averaged vibration level difference across the junction. The vibrational reduction index is measured by structural excitation and calculated by normalizing the direction averaged vibration level difference over the junction: (7) (9)

$$K_{ij} = D_{v,ij} + 10log10\left(\frac{l_{ij}}{\sqrt{a_i a_j}}\right) \tag{2.28}$$

Where $D_{v,ij}$ is the direction averaged vibration level difference in decibels, $l_{ij}$ is the junction length in meters, $a_i$ and $a_j$ are the equivalent absorption lengths expressed in meters which is related to the structural reverberation time $T_s$ of element $i$ and $j$: (9)

$$a_i = \frac{2.2\pi^2 S_i}{T_{s,i} c_0 \sqrt{\frac{f}{f_{ref}}}} \tag{2.29}$$

Where $S_i$ is the surface area of element i in square meters, $T_{s,i}$ is the structural reverberation time of element $i$ in seconds, $c_0$ is the speed of sound in air in $m/s$, $f$ is the frequency and $f_{ref}$ is the reference frequency which in this case is 1000 Hz. (9)

**Direction average velocity level difference.**

$\overline{D_{v,ij}}$ is the average velocity level difference over a junction between two elements in both directions which can be calculated as:

$$\overline{D_{v,ij}} = \frac{1}{2}\left(D_{v,ij} + D_{v,ji}\right) \tag{2.30}$$

Where $D_{v,ij}$ / $D_{v,ji}$ is the level difference of time and space averaged mean squared normal velocity over element $i/j$ and $j/i$ when only element $i$ or $j$ is excited.
The velocity level difference between element i and j can be calculated as:

$$D_{v,ij} = L_{vi} - L_{vj} \tag{2.31}$$

Where $L_{vi}$ is the average velocity level.
For air borne or steady state structure borne excitation the average velocity level is calculated as following:

$$L_v = 10\log\left(\frac{\frac{1}{T_{int}}\int_0^{T_{int}}\sum_{n=1}^{n} v_n^2(t)dt}{nv_0^2}\right) \tag{2.32}$$

Where $T_{int}$ is the integration time in seconds, $v_n$ is the r.m.s velocities in m/s at n different measurement points, $v_0$ is the reference velocity ($v_0 = 10^-9$ m/s).

For transient structure borne excitation the normal velocity is measured, then $D_{v,ij}$ is calculated as:

$$D_{v,ij} = \frac{1}{MN}\sum_{m=1}^{M}\sum_{n=1}^{N}(D_{v,ij})_{mn} \tag{2.33}$$

Where M is the number of excitation points on the element, N is the number of excitation points on the element, $(D_{v,ij})_{mn}$ is the velocity difference for one excitation of a pair of measurement points that can be calculated as: (9)

$$(D_{v,ij})_{mn} = 10log\left(\frac{\int_0^{T_{int}} v_{i,mn^2}(t)(dt)}{\int_0^{T_{int}} v_{j,mn^2}(t)(dt)}\right) \tag{2.34}$$

### 2.4.1 Structural reverberation time

The reverberation time (RT) of a structure was determined using frequency response function measurements. Initially, the acceleration data from excitation points was transformed to the time domain using an inverse Fourier transform. The time-domain signals were then used to calculate energy decay curves, obtained by computing the cumulative sum of the squared signals, followed by converting the results to decibels (dB). To estimate the reverberation time, a linear regression was performed on a selected portion of the decay curve. The slope from this regression represented the rate of energy decay in dB per second. Finally, the reverberation time was calculated using the formula:

$$RT_{60} = \frac{-60}{K_1} \tag{2.35}$$

Where $K_1$ is the slope of the linear regression fit on the decay curve.

# Chapter 3

# Measurements

## 3.1 Equipment

The equipment used for the measurements were:

- One-axis accelerometers
- Impact hammer
- Christian Berners angle iron (GePi100)
- Measurement system Siemens LMS Scadas III

Figure 3.1: Impact hammer


Figure 3.2: Accelerometer

Figure 3.3: Equipment used for the measurements.


Figure 3.4: Measurement system Siemens LMS Scadas III.

## 3.2 Measurement setup and limitations

### 3.2.1 Limitations

For this measurement set-up the walls had to be mounted in supports due to safety reasons and ease of disassembly. The assembly itself was done by the staff at the lab. This should not impact the results to much as the assembly is not complicated. With a structure this big it was not possible to have it hanging from ropes to decouple it from the ground completely, instead the use of Sylomere was used in order to try to decouple the structure from ground vibrations.

### 3.2.2 Measurement rig

The measurements were carried out on a structure that was comprised of one 5 layer panel with the dimensions: 2.7 m x 3 m, two 3 layer panels 2.7 m x 3 m and one 3 layer panel 6 m x 3 m. The assembled structure can be seen below3.7.

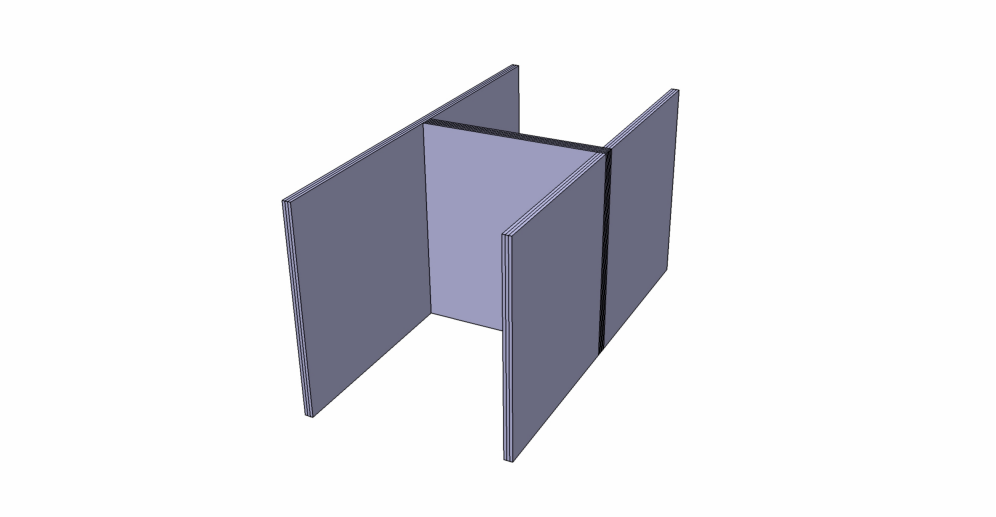

Figure 3.5: Measurement rig modeled in Catia.

### 3.2.3 Measurement without vibration isolation solution

The first measurement was done in order to determine the material parameters. The panel was suspended in mid-air using an overhead crane and ropes to simulate free boundary conditions. Three accelerometers were then placed on the CLT-panel; this was done according to ISO 10848-1:2017. An impact hammer with a force sensor was then used to excite the panel, ten hits were done for each measurement. This was done in order to get the impulse response and frequency response function for the three-layered and five-layered panels.(7) (8)

The second measurement was done when the panels were mounted in the supports but still not connected to each other. (see Figure below). Five accelerometers were then mounted to the structure and two excitation points were also mapped out. An impact hammer was then used to excite the panel ten times per excitation point. The impact hammer was connected to the SIEMENS LMS system, which handled the data and calculated the FRF.

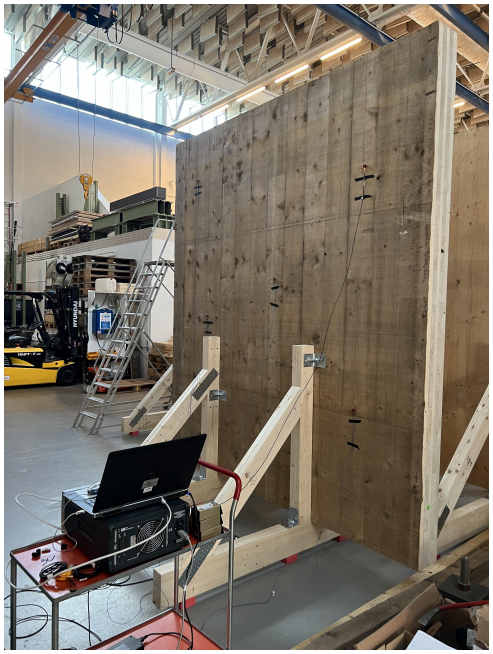

Figure 3.6: CLT-panel mounted to support structure.

This was in order to see if the supports had any effect on the structure. After the initial measurements the structure was put together according to the construction documentation. This was done without any kind of vibrational isolating material (see figure below) 3.7.

Figure 3.7: Structure without vibrational dampening material.

With the structure in place, five one-axis accelerometers were placed in random spots across the surface of three of the panels, as can be seen in the picture below. Each spot was marked with M1, M2... and so forth to make sure that the measuring points did not change between the measurements. The spots were also matched with a certain accelerometer to make sure the same accelerometer was used for e.x. Measurement point one (M1) each time.
In this set-up, fifteen accelerometers were used in total. Three different panels were prepared for each measurement, with the floor having its accelerometers mounted on it at all times. The first measurement included wall 1 and 4 (see figure 3.8) as well as the floor panel.

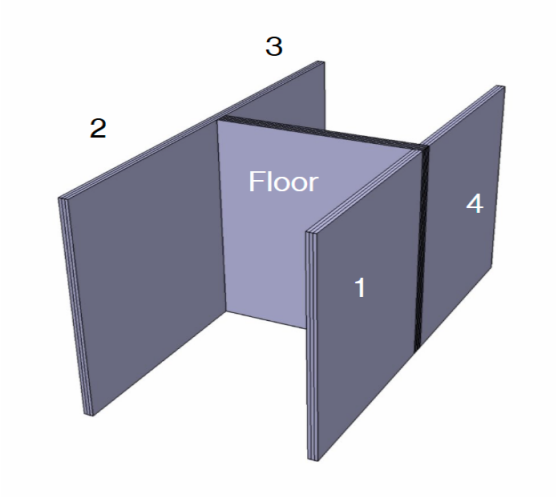


Figure 3.8: 3D Render of structure with numbered walls.

When all the accelerometers were securely mounted to the panels, one panel was excited at a time with an impact hammer. The excitation of the panels was done ten times per excitation point with two excitation points per panel. This procedure was done in sets of two, first the floor and wall one and then the floor and wall four and lastly wall one and four.
The same procedure was done for the other half of the measurement rig, the floor and wall two and three.

The data from the measurements was then handled by the SIEMENS system which provided a frequency response function from 1 Hz to 3200 Hz

Figure 3.9: Accelerometers mounted on the panels.

### 3.2.4 Measurement with GePi100.

After the measurement of the first assembly of the panels, they were deconstructed and a vibrational dampening solution was applied. The solution in this case was Christian Berners GePi100 (see figure 3.10)

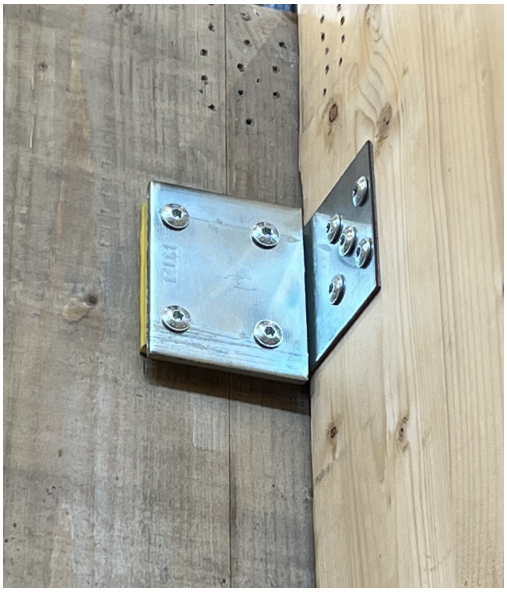

Figure 3.10: Christian Berner's Gepi100.

The GePi100 was mounted between the floor and wall one and also between the floor and wall two (and three). Three GePi100 brackets were used for each connection (see figure below 3.11). I also made sure that there was a gap between the panels where the mounts where attached so that they were only coupled through the angle irons (GePi100). After that the accelerometers were mounted on the panels again in the same exact way as they were before. The measurements where then done again with the same excitation points as the previous measurements.

Figure 3.11: Christian Berners GePi100 mounted on the CLT-structure.

# Chapter 4

# Finite element method

## 4.1 Initial model

The initial stage of the finite element method (FEM) employed a simplified model as the foundation of analysis. This simplified model consisted of a simply supported plate with specific dimensions:0.3 m in length, 0.2 m in width, and 0.01 m in depth, as illustrated in Figure 4.1. The material parameters were chosen to correspond to those of spruce. The mesh was set to the extra fine option in COMSOL and the face meshing method was set to Quadrilateral (see figure 4.2).
To emulate the behavior of a simply supported plate, boundary conditions were set to be fixed along the middle of the sides of the plate (see figure 4.1).
It is noteworthy that the decision to model the plate as a solid, rather than as a shell was to make the model behave more like the real real life structure. The adoption of a solid model aligns with the 3D nature of the subsequent modeling tasks.
As a means of validation, the correctness of the FEM model was assessed by comparing the computed eigenfrequencies with analytical values 4.1. These analytical values were derived utilizing relevant equations, which are referenced as Equation 2.21.
This approach ensured the accuracy and reliability of the FEM model in simulating the vibrational behavior of the simply supported Isotropic plate.

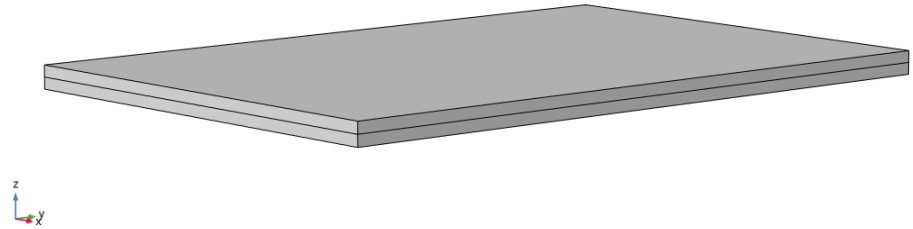

Figure 4.1: Simply supported spruce plate made in Comsol.

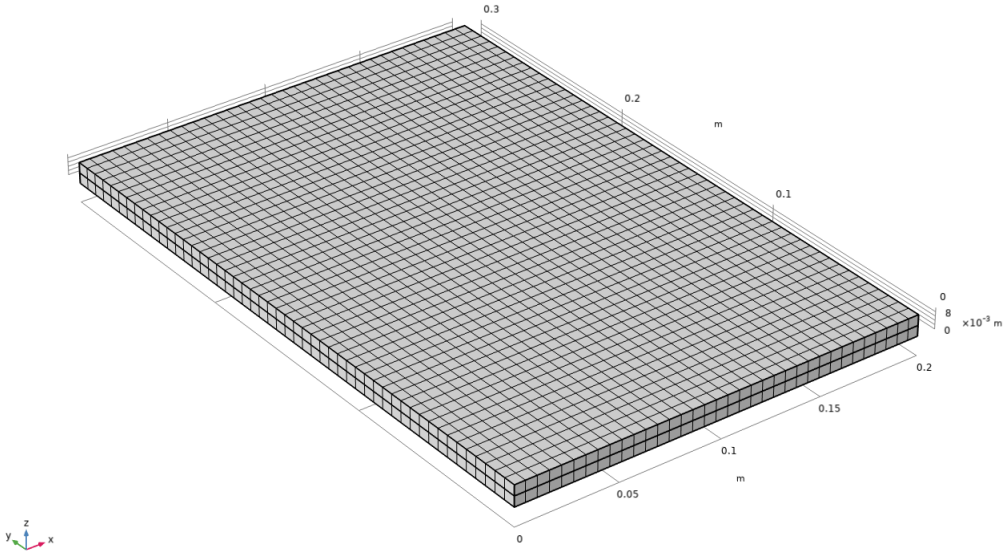


Figure 4.2: Mesh of the spruce plate in Comsol.

| Analytical values (isotropic plate) | FEM values (isotropic plate) |
|---|---|
| 741 Hz | 727.5 Hz |
| 1425 Hz | 1391 Hz |
| 2280 Hz | 2228 Hz |
| 2565 Hz | 2493 Hz |
| 2964 Hz | 2862.5 Hz |
| 4104 Hz | 3926.5 Hz |
| 4161 Hz | 4010.5 Hz |
| 4845 Hz | 4087.3 Hz |
| 5528 Hz | 4661.8 Hz |
| 5699 Hz | 5265 Hz |

Table 4.1: Comparison of eigenfrequencies from analytical method to Comsol for an isotropic plate.

The same model was then used but with orthotropic properties instead. The material properties were set to be the same as for an isotropic plate, namely the same properties in all directions, this was done in order to validate the orthotropic model compared with the isotropic plate.

## 4.2 Full scale model

The full scale model that is meant to represent the physical panels that the measurements are made on was first modeled in the Catia software to be able to accurately depict the physical object. The choice of Catia over COMSOL was made because COMSOL's modeling capabilities are relatively limiting compared to other software options.
This was done for two different configurations: T-junction and X-junction (see figure4.5, 4.8). These configurations were also made with and without brackets.

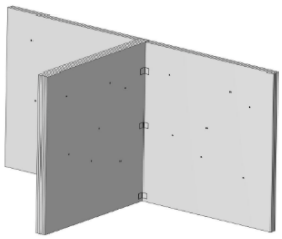

Figure 4.3: X-junction.

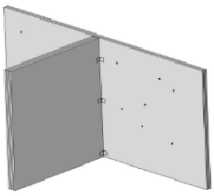

Figure 4.4: T-junction.

Figure 4.5: COMSOL models of X and T junction.

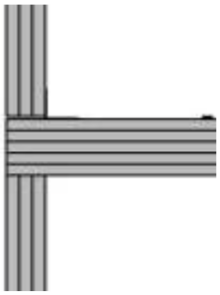

Figure 4.6: X-junction.

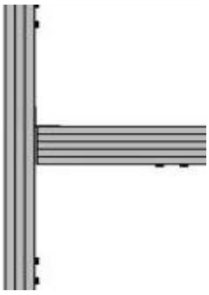

Figure 4.7: T-junction.

Figure 4.8: Top view of the X and T junctions.

The model made in Catia was then imported to COMSOL as an stp file to be able to continue with the FEM simulations. When imported the model was assigned materials with linear elastic, anisotropic properties for each of the parts. Each panel was given the material parameters according to the directions of the grains, with each panel having the grains in the opposite direction to the next, for example: grains going in X-direction, Y-direction then X-direction.
The Poisson's ratio together with the shear modulus and Young's modulus was then applied to the three different directions of the model. These values where fetched from Södras data sheet and applied according to the class of CLT panel (10). Poisson's ratio was assumed to be that of wood (6). The density of the panels was aquiered by weighing the panels in the overhead crane. The loss factor for Young's Modulus was also set according to the measurement which was obtained by calculating the reverberation time from the measurement and then using equation below and the loss factor for the shear modulus was assumed to be the same.

$$\eta = \frac{2.2}{T_s * f} \tag{4.1}$$

Where $T_s$ is the structural reverberation time and $f$ is the frequency.

| | |
|---|---|
| $E_X$ | 11.17 GPa |
| $E_Y$ | 0.43 GPa |
| $E_Z$ | 7.733 GPa |
| $G_{XY}$ | 0.43 GPa |
| $G_{XZ}$ | 0.139 GPa |
| $G_{YZ}$ | 0.192 GPa |
| $\mu_{LR}$ | 0.40 |
| $\mu_{RT}$ | 0.30 |
| $\mu_{LT}$ | 0.35 |
| $\rho$ | 455 kg/m$^3$ |
| $\eta_E$ | 0.3803 |
| $\eta_G$ | 0.3803 |

Table 4.2: Material parameters for CLT 120mm 3-layer.

| | |
|---|---|
| $E_X$ | 9.395 GPa |
| $E_Y$ | 2.205 GPa |
| $E_Z$ | 6.716 GPa |
| $G_{XY}$ | 0.466 GPa |
| $G_{XZ}$ | 0.141 GPa |
| $G_{YZ}$ | 0.090 GPa |
| $\mu_{XY}$ | 0.40 |
| $\mu_{XZ}$ | 0.30 |
| $\mu_{YZ}$ | 0.35 |
| $\rho$ | 455 kg/m$^3$ |
| $\eta_E$ | 0.6498 |
| $\eta_G$ | 0.6498 |

Table 4.3: Material parameters for CLT 190mm 5-layer.

To simulate the impact of the measurement a point load of $-1$ N was applied perpendicular to the CLT element at the same excitation points as the measurement. Measurement points were set for each panel to mirror

that of the measurement with five points for each panel. The boundary conditions for the different elements was set to free to simulate the structure being de coupled from the ground as well as not being fixed in any corners as it was during the measurements.
Another model was also used with the vibration reduction brackets from Christian Berner (GePi100) in between the floor and wall one. The setup was the same as the simulation before with one difference, the surface where the brackets and the floor panel meet the function ”elastic thin layer” was used to simulate the Sylodyn used in GePi100. The material parameters for this material was found on Christian Berners website (Berner). Youngs modulus of the Sylodyn was then increased from 1.32 GPa to 7.32 GPa to try and simulate the tension that the screws mounting the bracket to the panel would cause. This was done because the initial value of 1.32 GPa did not match the measured results.
Another setup was used where an extra feature, called ”bolt pretension,” was added to the underside of the brackets where they connect to the floor. In this configuration, a pressure of $1\,\mathrm{N/m^2}$ was applied.

# Chapter 5

# Results and discussion

### 5.0.1 Results of the structure without GePi100 installed.

The graphs below show the results gathered from the measurement of the structure with no vibration dampening brackets being used. In the plot one can see that the simulated $K_{ij}$ follows the trend of the measured $K_{ij}$ to a certain degree although it does not show the does not show the resonance frequencies that well. This might be because the resolution of the measured results are much higher then that of the simulated results.

Another reason for this might be that the supports that were used during the measurements where not modeled in Comsol, which might have contributed to larger resonances.

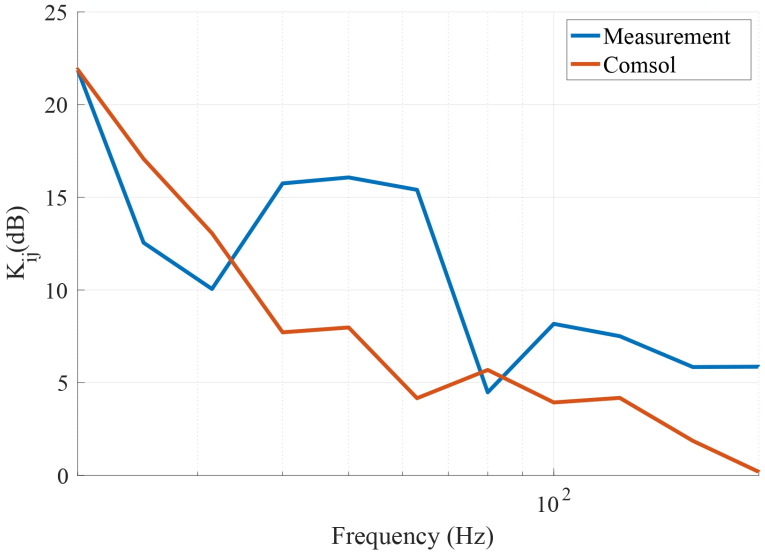


Figure 5.1: $K_{ij}$ of floor to wall 1 in 1/6th octaves.

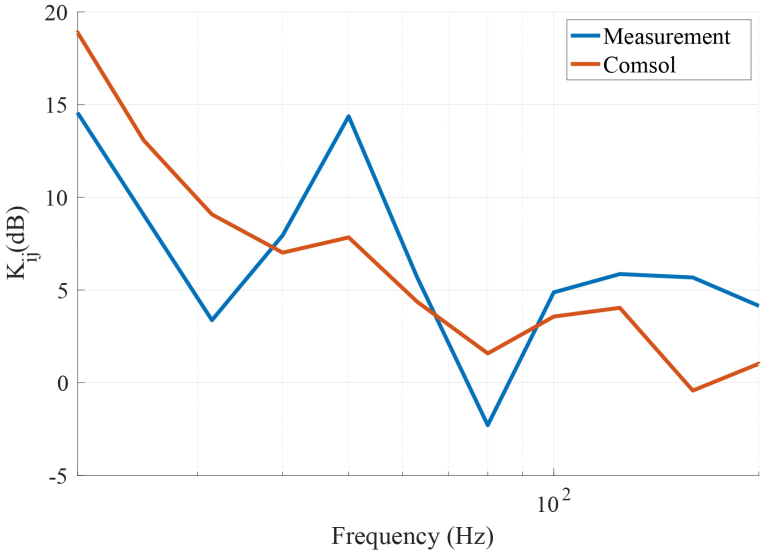


Figure 5.2: $K_{ij}$ of floor to wall 4 in 1/6th octaves

Figure 5.3: $K_{ij}$ from measurement and simulation of floor to wall 1 and 4.

The simulation results of the floor to wall 3 5.6 also follows the trend of the measured result quite well but shows a significant reduction in $K_{ij}$ this might be due to the simulation model assuming that the different panels were joint together while in the measured results the panels were screwed together which might not have been good enough causing the panels to not be coupled together as well as they are in the simulated result.

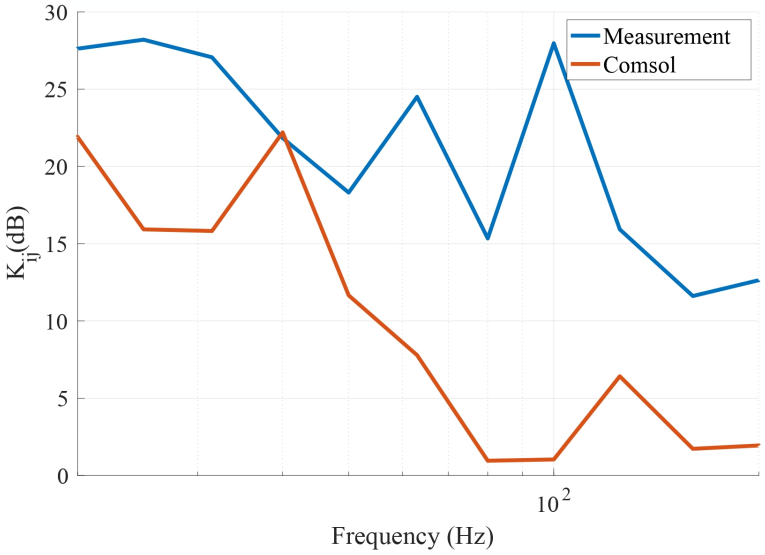


Figure 5.4: $K_{ij}$ of floor to wall 2 in 1/6th octaves.

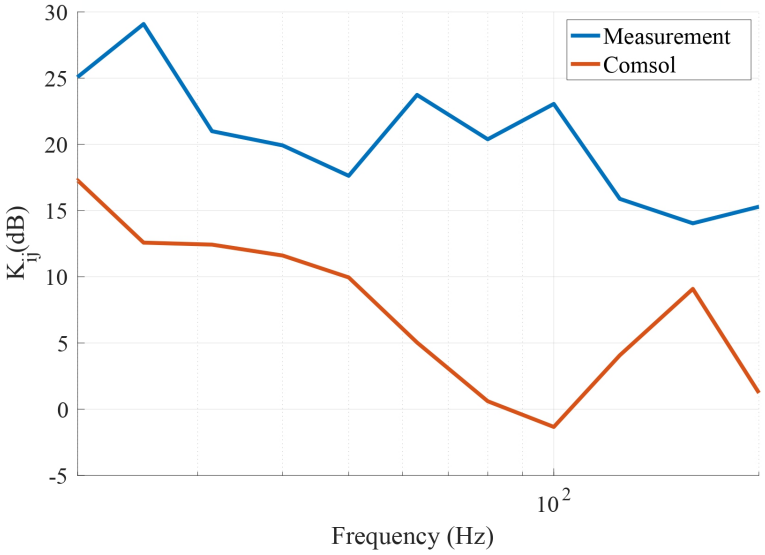


Figure 5.5: $K_{ij}$ of floor to wall 3 in 1/6th octaves

Figure 5.6: $K_{ij}$ from measurement and simulation of floor to wall 2 and 3.

In the results from wall 1 to wall 4 the trends are quiet similar but it looks like the coupling between the panels for the measured result is not as strong as it is in the simulated results which causes a higher $K_{ij}$ for the measured result.

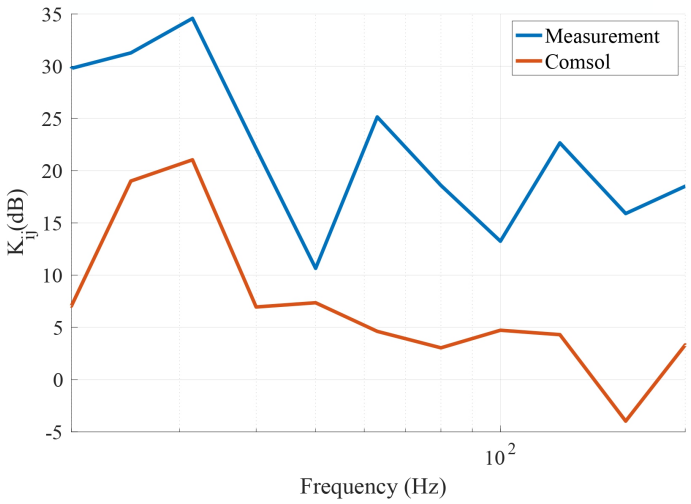


Figure 5.7: $K_{ij}$ of wall 1 to wall 4 in 1/6th octaves.

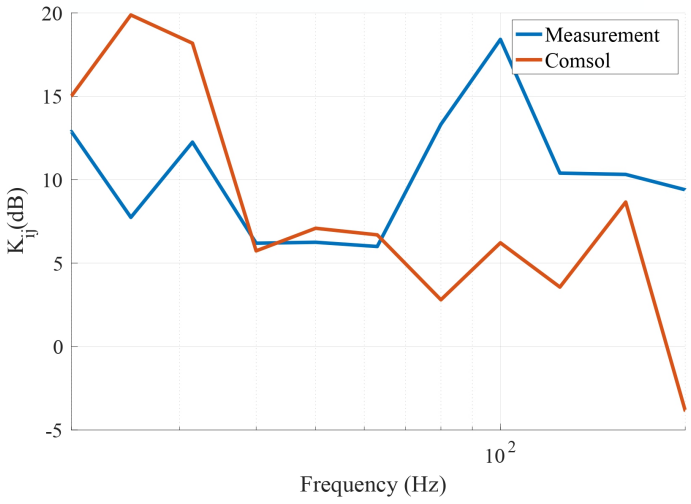


Figure 5.8: $K_{ij}$ of wall 2 to wall 3 in 1/6th octaves

Figure 5.9: $K_{ij}$ from measurement and simulation of wall 1 to 4 and wall 2 to 3.

### 5.0.2 Results of the structure with GePi100 installed.

In the results of the structure with GePi100 installed and the simulation results using the thin elastic layer function the trend is quiet similar to each other with a clear level difference of $K_{ij}$ with the simulated value being a lot higher in certain areas. This might be because the thin elastic layer causes to much decoupling between the bracket and the CLT-panel which causes $K_{ij}$ to be much higher than it should be as less of the vibrations can propagate through to the other panel. This trend of higher $K_{ij}$ is prevalent in all simulations done with thin elastic layer as can be seen in the figures down below.
The results are only valid for this specific measurement rig and assembly. The measured data cannot be used as product specifications for GePi100 when installed in a building.

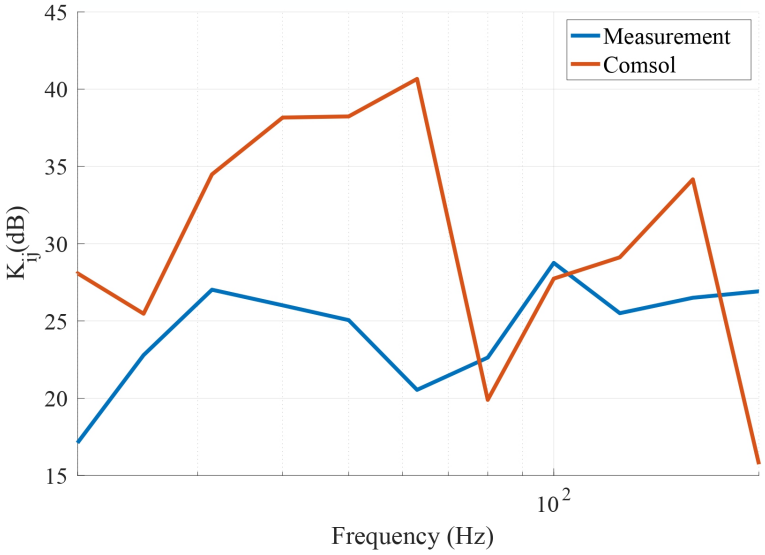


Figure 5.10: $K_{ij}$ of floor to wall 1 in 1/6th octaves with GePi100.

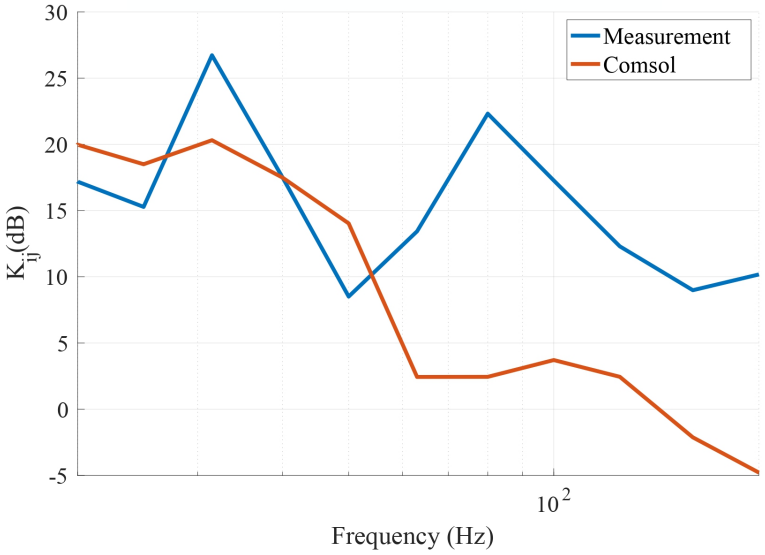


Figure 5.11: $K_{ij}$ of floor to wall 4 in 1/6th octaves with GePi100.

Figure 5.12: $K_{ij}$ from measurement and simulation with thin elastic layer of floor to wall 1 and wall 4.

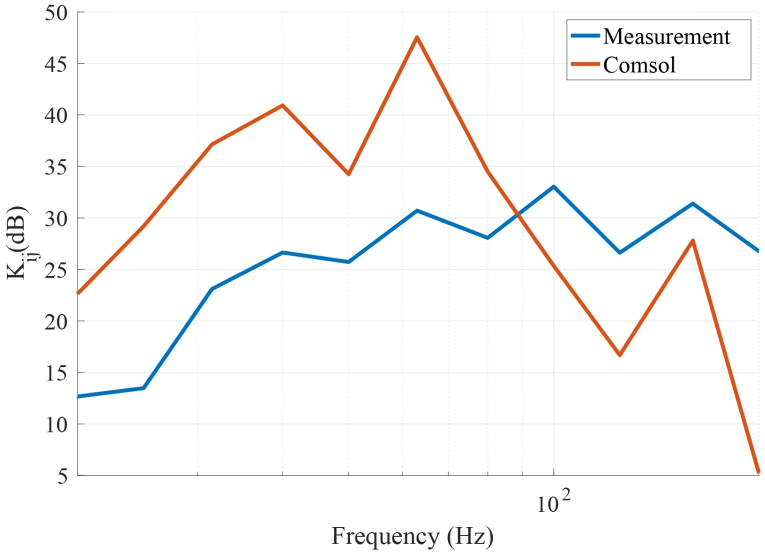


Figure 5.13: $K_{ij}$ of floor to wall 2 in 1/6th octaves with GePi100.

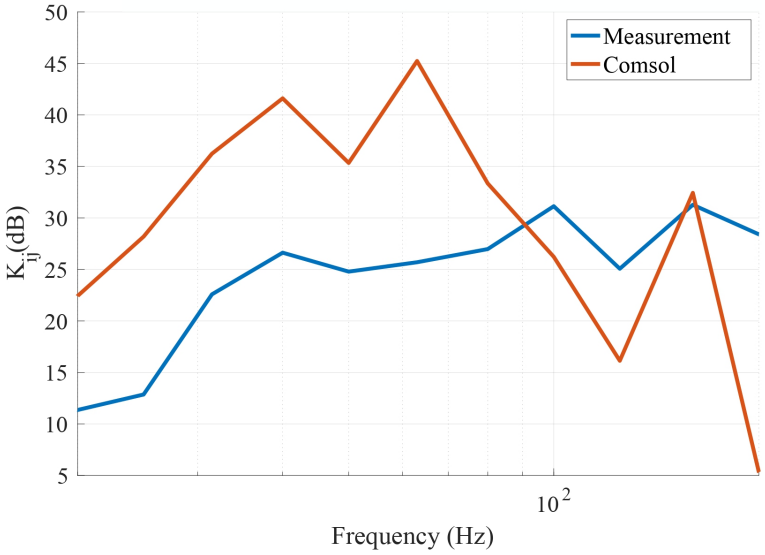


Figure 5.14: $K_{ij}$ of floor to wall 3 in 1/6th octaves with GePi100.

Figure 5.15: $K_{ij}$ from measurement and simulation with thin elastic layer of floor to wall 2 and wall 3.

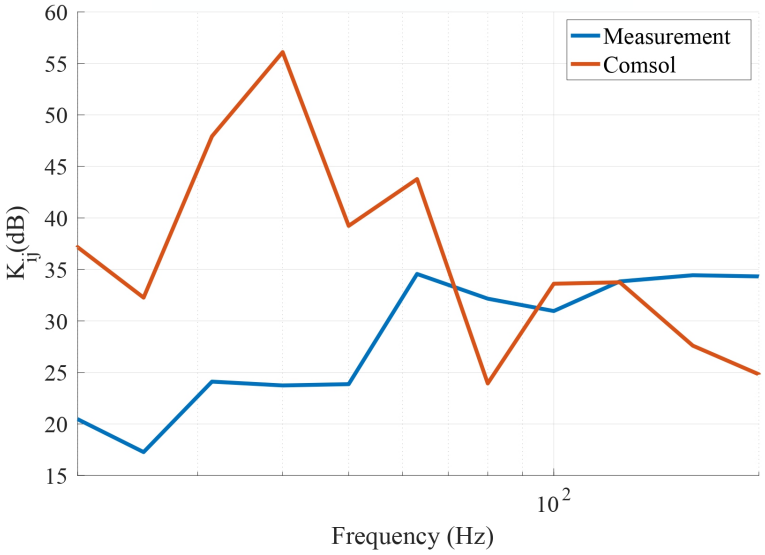


Figure 5.16: $K_{ij}$ of wall 1 to wall 4 in 1/6th octaves with GePi100.

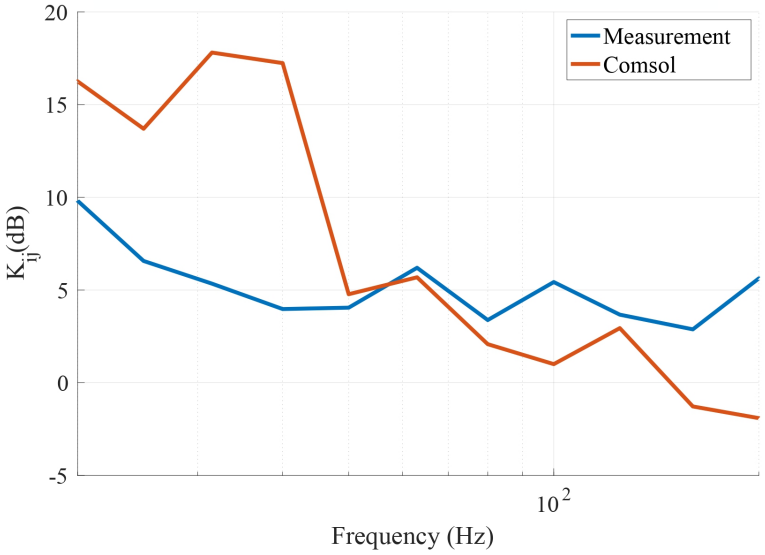


Figure 5.17: $K_{ij}$ of wall 2 to wall 3 in 1/6th octaves with GePi100.

Figure 5.18: $K_{ij}$ from measurement and simulation with thin elastic layer of wall 1 to wall 4 and wall 2 to wall 3.

In the other variation of the simulation the brackets where modeled with both the thin elastic layer and bolt pretension functions in order to try to

make the coupling stronger between the panels while still having the thin elastic layer to dampen the vibrations. This configuration resulted in too much coupling and the structure behaved more closely to that of the structure when the GePi100 brackets where not mounted as can be seen in the figures below.

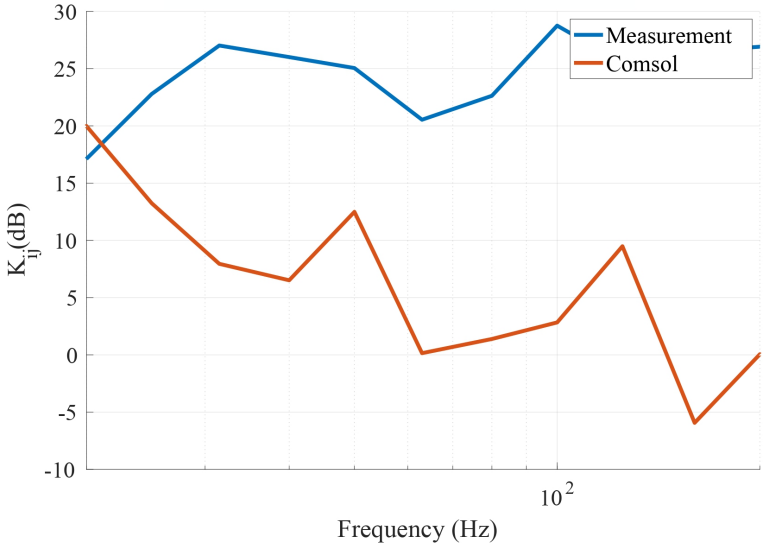


Figure 5.19: $K_{ij}$ of floor to wall 1 in 1/6th octaves with GePi100.

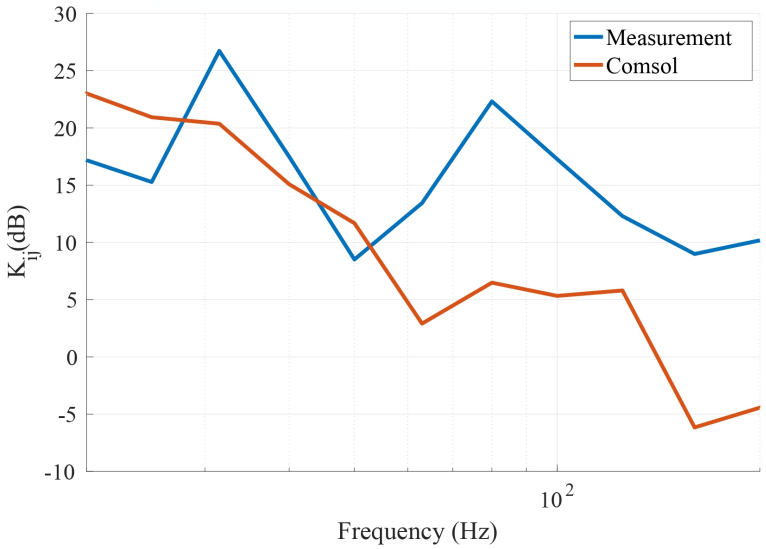


Figure 5.20: $K_{ij}$ of floor to wall 4 in 1/6th octaves with GePi100.

Figure 5.21: $K_{ij}$ from measurement and simulation with thin elastic layer and bolt pretension of floor to wall 1 and wall 4.

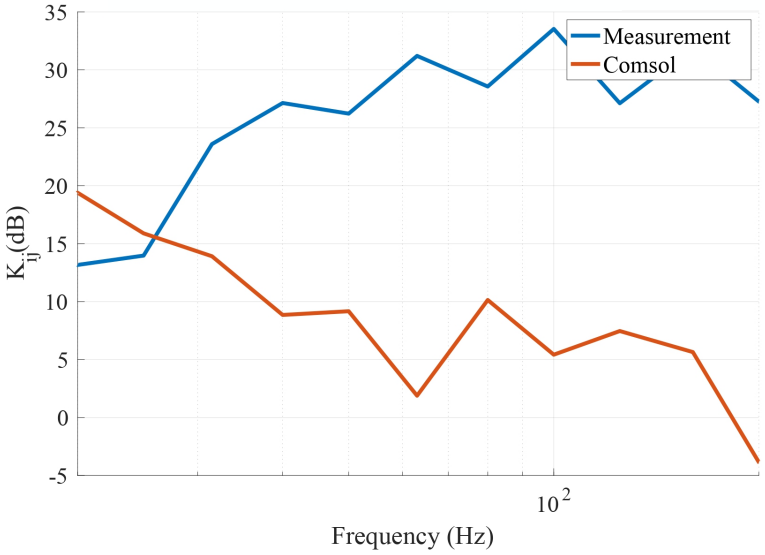


Figure 5.22: $K_{ij}$ of floor to wall 2 in 1/6th octaves with GePi100.

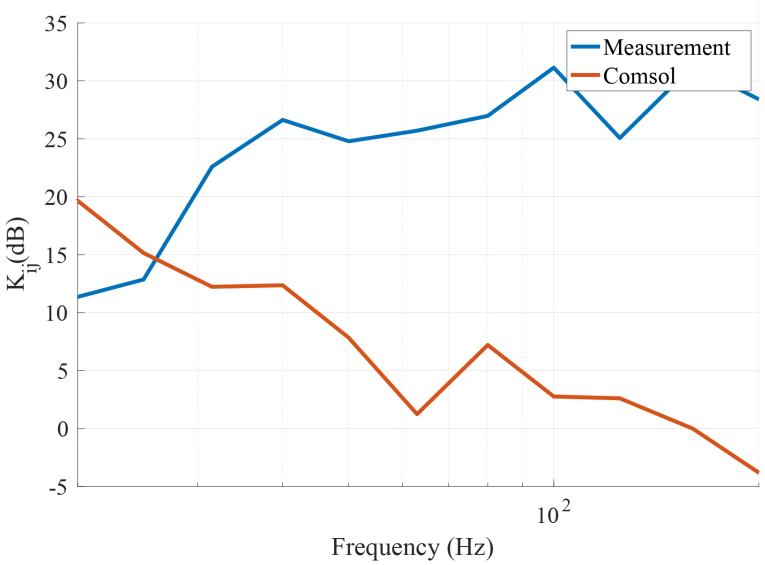


Figure 5.23: $K_{ij}$ of floor to wall 3 in 1/6th octaves with GePi100.

Figure 5.24: $K_{ij}$ from measurement and simulation with thin elastic layer and bolt pretension of floor to wall 2 and wall 3.

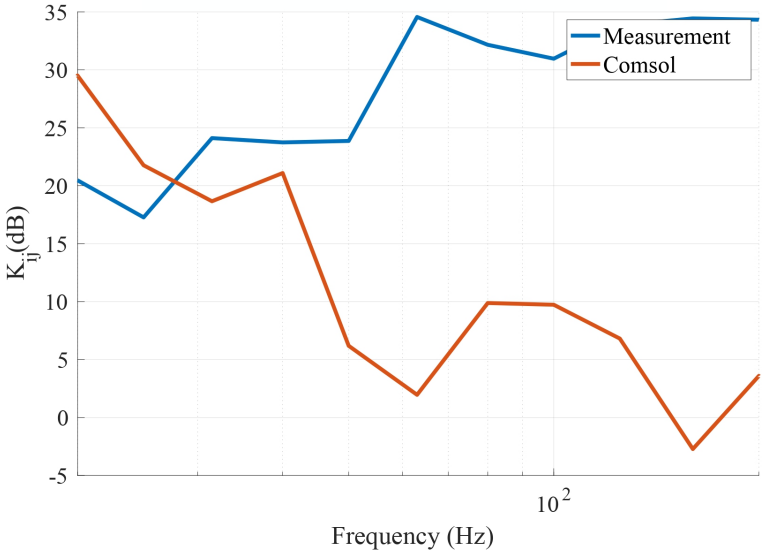


Figure 5.25: $K_{ij}$ of wall 1 to wall 4 in 1/6th octaves with GePi100.

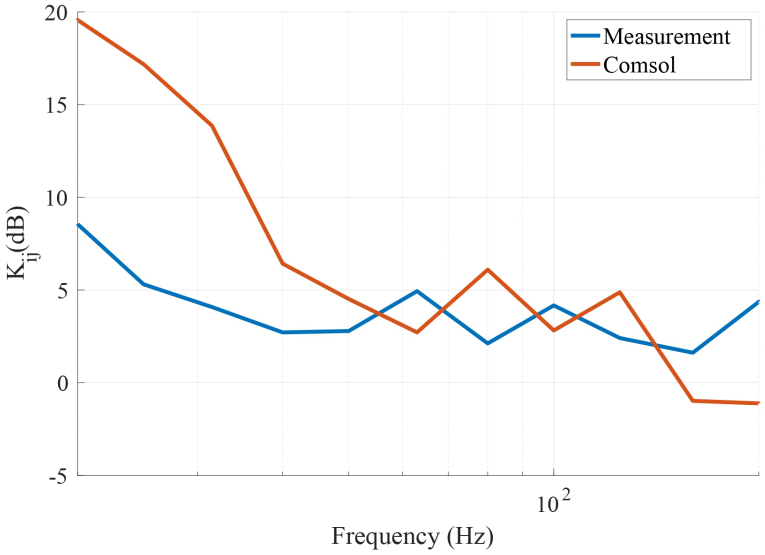


Figure 5.26: $K_{ij}$ of wall 2 to wall 3 in 1/6th octaves with GePi100.

Figure 5.27: $K_{ij}$ from measurement and simulation with thin elastic layer of wall 1 to wall 4 and wall 2 to wall 3.

# Chapter 6

# Conclusion and future works

### 6.0.1 Conclusion

**Structure without vibration dampening brackets**

For the structure without GePi100 brackets, the simulated values of $K_{ij}$ followed the trends of the measured results fairly well. However, there were some differences between the two. One reason for this might be how the structure was built for the measurements compared to how it was modeled in COMSOL. The way the panels were joined and coupled during the experiment may not have been the same as in the model. Another reason could be the resolution of the data. The measurements were done at a much higher resolution than the simulations, which may have caused some variation in the results. These issues show that while the model worked to some extent, there is room for improvement to make it match the measurements more accurately.

**Structure with vibration dampening brackets**

When the GePi100 vibration dampening brackets were installed, the results from the simulations did not match the measured values. The model either overestimated or underestimated $K_{ij}$, depending on how the coupling between the panels was simulated. This suggests that the current way of modeling the brackets in COMSOL is not accurate enough. It is likely that the interaction between the brackets, the dampening material, and the CLT panels is more complex than the model assumes. This area needs more attention in future studies.

### 6.0.2 Future works

To improve these results, future work should focus on a few key areas:

**Better Modeling of Panel Coupling.**
The way the panels are joined together needs to be modeled with more details in mind. The coupling between the panels plays an important role in how vibrations move through the structure, so better simulations are needed to reflect this.

**Improving Bracket Modeling.**
The vibration dampening brackets need to be modeled in a way that better reflects how they behave in real life. This includes accounting for how the dampening material reacts to being mounted with screws and how it interacts with the panels. It is important to find a balance between decoupling vibrations and keeping the panels properly connected.

**Revisiting the Measurement Setup.**
The experimental setup could also be improved. During the measurements, the panels were mounted on supports, which may have affected the results. A better way to measure would be to suspend the structure in the air to create free boundary conditions. If that isn't possible, it would help to model the supports in a way that does not make the simulations take too long.

**Higher resolution Simulations.**
Future simulations should use higher resolution to better match the level of detail in the measurements. This would help capture things like resonance frequencies more accurately.

By working on these areas, future studies can improve the accuracy of the simulations and make them more reliable. This would make it easier to predict the vibration behavior of CLT structures, especially for practical use in construction.

# Bibliography

[Berner] Berner, C. Sylodyn. https://www.christianberner.se/globalassets/leverantorer/getzner-werkstoffe-gmbh/dokument/sylodyn.pdf.

[2] Cremer, L., Heckl, M., and Petersson, B. A. T. (2005). *Structure-borne sound: Structural vibrations and sound radiation at audio frequencies*. Springer.

[3] Gustafsson, A. (2019). The cltt handbook. `https://www.swedishwood.com/siteassets/5-publikationer/pdfer/clt-handbook-2019-eng-m-svensk-standard-2019-2022.pdf`. [Accessed 14-01-2025].

[4] Hopkins, C. (2007). *Sound Insulation — Carl Hopkins — Taylor & Francis eBooks, Reference W — doi.org*. [Accessed 14-01-2025].

[5] Kropp, W. (2015). Propagation and radiation of structure borne sound.

[6] Sonelastic® (2024). Woods elastic modulus and poisson ratio. Accessed: 2024-11-12.

[7] Swedish standard institute (2017a). Acoustics – laboratory and field measurement of flanking transmission for airborne, impact and building service equipment sound between adjoining rooms – part 1: Frame document (iso 10848-1:2017). Standard ISO 10848-1:2017, Swedish standard institute, Geneva, CH.

[8] Swedish standard institute (2017b). Acoustics – laboratory and field measurement of flanking transmission for airborne, impact and building service equipment sound between adjoining rooms – part 4: Application to junctions with at least one type a element (iso 10848-4:2017). Standard ISO 10848-4:2017, Swedish standard institute, Geneva, CH.

[9] Swedish standard institute (2017c). Building acoustics – estimation of acoustic performance of buildings from the performance of elements – part 1: Airborne sound insulation between rooms (iso 12354-1:2017). Standard ISO 12354-1:2017, Swedish standard institute, Geneva, CH.

[10] Södra (2024). Product properties of södra's clt wood. Accessed: 2024, PDF document.

[11] Vigran, T. E. (2014). *Building Acoustics.* CRC Press.

# Appendix A

# Pictures

## A.1 Assembly instructions for measurement rig

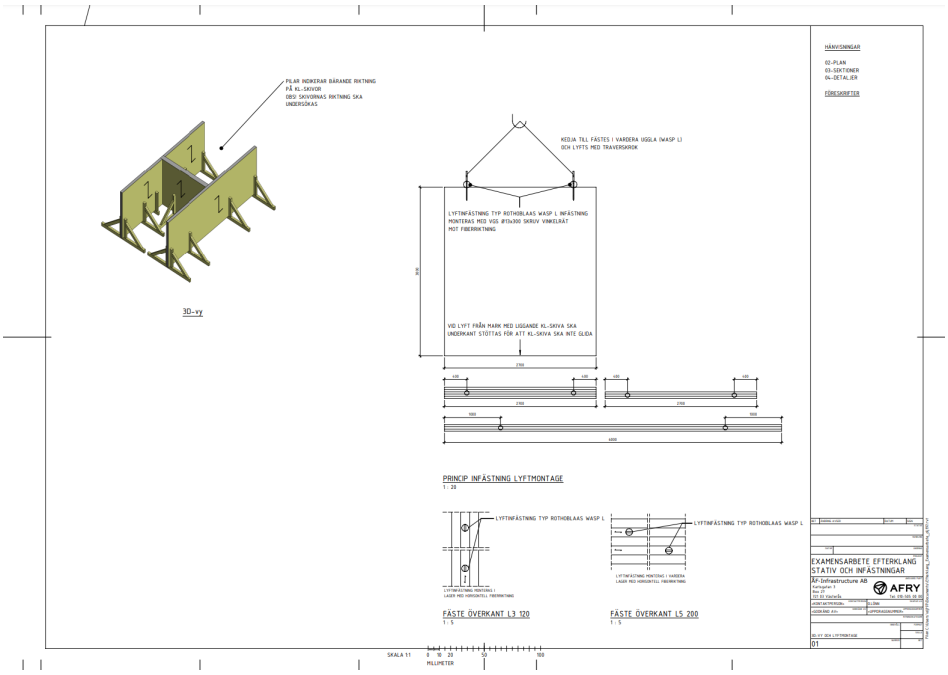


Figure A.1

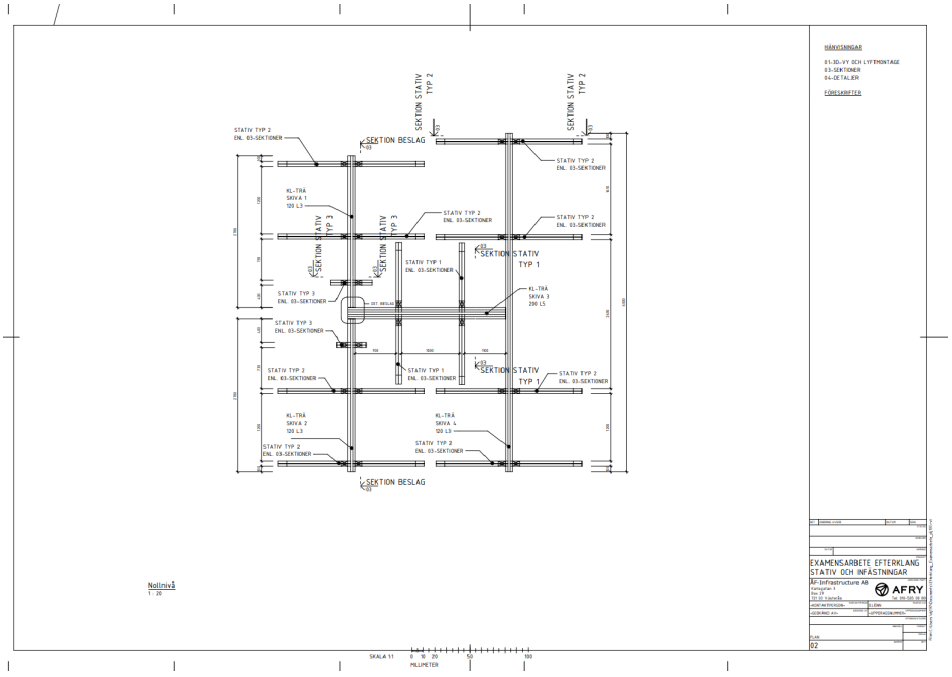


Figure A.2

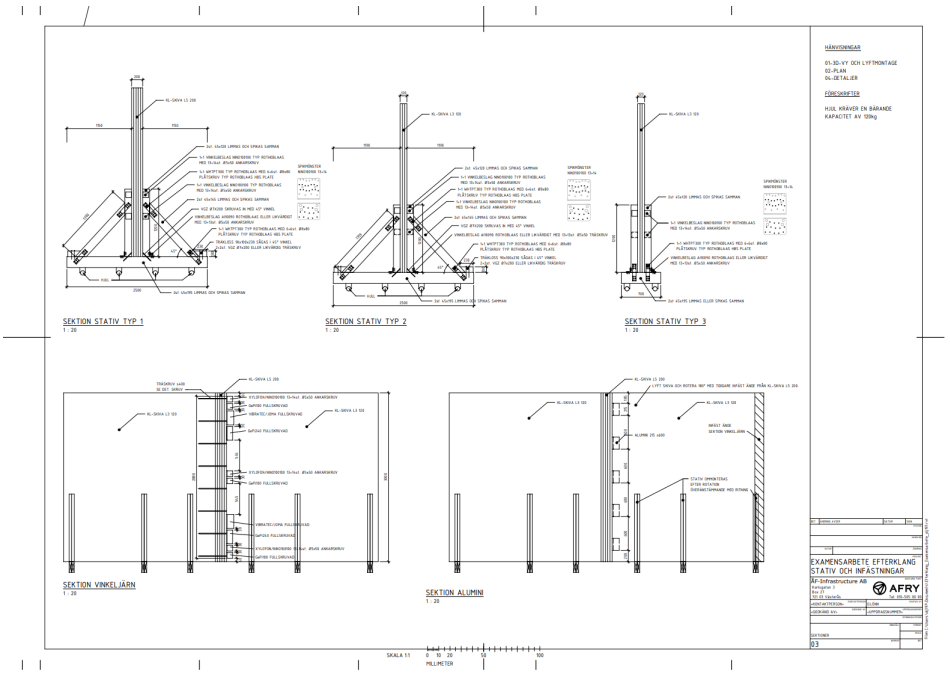


Figure A.3

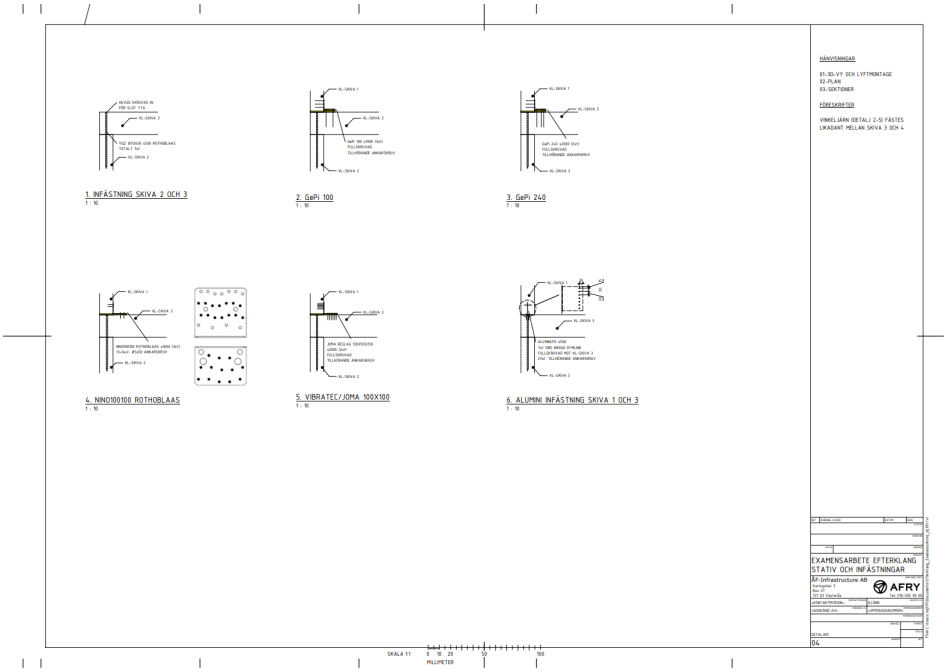
HÄNVISNINGAR
01-3D-VY OCH LYFTMONTAGE
02-PLAN
03-SEKTIONER
FÖRESKRIFTER
VINKELJÄRN (DETALJ 2-5) FÄSTES
LIKADANT MELLAN SKIVA 3 OCH 4
1. INFÄSTNING SKIVA 2 OCH 3
1 : 10
2. GePi 100
1 : 10
3. GePi 240
1 : 10
4. NINO100100 ROTHOBLAAS
1 : 10
5. VIBRATEC/JOMA 100X100
1 : 10
6. ALUMINI INFÄSTNING SKIVA 1 OCH 3
1 : 10
EXAMENSARBETE EFTERKLANG
STATIV OCH INFÄSTNINGAR
ÅF-Infrastructure AB
AFRY
SKALA 1:1
0 10 20 50 100
MILLIMETER
04

Figure A.4